Journal of Ceramic Processing Research. Vol. 26, No. 1, pp. 117~121 (2025)
(Received 8 November 2024, Received in revised form 1 February 2025, Accepted 5 February 2025)
https://doi.org/10.36410/jcpr.2025.26.1.117

J O U R N A L O F
Ceramic Processing Research

Comparative study of silicon nitride ceramics and pitta moluccensis humerus bone for bone substitution applications

Juan Chen[a,*] and Peng Guo[b]
[a]*Public Education Department, Zhumadian Preschool Education College, Zhumadian 463003, Henan, China*
[b]*College of Life Sciences, Henan Agricultural University, Zhengzhou 450046, Henan, China*

Silicon nitride (Si_3N_4) ceramics are emerging as promising materials for biomedical applications, particularly in bone tissue engineering, due to their outstanding mechanical properties, biocompatibility, and osteoconductivity. This study investigates the potential of Si_3N_4 ceramics by comparing their microstructure and mechanical properties with the demineralized humerus bone of *Pitta moluccensis*, a bird species known for its lightweight and robust skeletal structure. Using X-ray computed tomography and mercury intrusion porosimetry, the study found that Si_3N_4 ceramics exhibit a porosity of approximately 50 vol%, similar to the 70 vol% porosity in the bird bone. The Si_3N_4 ceramics demonstrated a hardness of 0.4 GPa, a Young's modulus of 15 GPa, and a compressive strength of 2.9±0.4 MPa, closely matching the 0.3 GPa hardness, 12 GPa Young's modulus, and 3.5 MPa compressive strength of the bird bone. These findings suggest that Si_3N_4 ceramics, with tailored porosity and mechanical properties, are a viable alternative for bone substitution, particularly in load-bearing applications.

Keywords: Osteointegration, Si_3N_4 ceramics.

Introduction

Silicon nitride (Si_3N_4) ceramics have emerged as a promising material in biomedical applications, particularly in orthopedic and dental fields, owing to their exceptional combination of mechanical properties, biocompatibility, and osteoconductive behavior. These ceramics address limitations associated with traditional biomaterials such as metals, polymers, and other ceramics, making them a compelling candidate for bone tissue engineering and implant design. The superior mechanical properties of Si_3N_4 ceramics, characterized by high fracture toughness, exceptional hardness, and remarkable wear resistance, render them suitable for load-bearing applications, such as in orthopedic implants. Unlike metallic implants, which are prone to corrosion and degradation in biological environments, Si_3N_4 exhibits chemical stability, minimizing long-term complications. Its low thermal expansion coefficient ensures dimensional stability under varying physiological conditions, further enhancing its suitability for long-term implantation.

In addition to these mechanical advantages, Si_3N_4 ceramics are inherently biocompatible and demonstrate osteoconductive behavior. These properties promote the attachment, proliferation, and differentiation of osteoblasts, facilitating integration with surrounding bone tissue and expediting healing processes. Furthermore, the antibacterial properties of Si_3N_4 ceramics, driven by their unique surface chemistry and ionic release mechanisms, reduce the risk of post-implant infections. This intrinsic antibacterial activity eliminates the need for extensive antibiotic use and significantly enhances implant longevity and patient outcomes.

In this study, the potential of Si_3N_4 ceramics as a biomimetic material is examined in the context of their comparison with the demineralized humerus bone of *Pitta moluccensis*, a bird species whose skeletal structures are characterized by high porosity and optimized mechanical properties for flight. Bird bones, such as the humerus of *Pitta moluccensis*, exhibit a unique combination of lightweight architecture and structural strength, making them a natural benchmark for biomaterial design. By investigating the microstructure, porosity, and mechanical behavior of demineralized bird bone alongside Si_3N_4 ceramics, this research aims to identify synergies and divergences in their properties, particularly in the context of osteogenesis and structural functionality. Through this comparative study, we aim to deepen the understanding of how Si_3N_4 ceramics can be engineered to emulate or surpass the biological and mechanical performance of natural bone. Moreover, leveraging advanced techniques such as mercury intrusion porosimetry, scanning electron microscopy, and additive manufacturing, the study explores the feasibility of creating Si_3N_4 scaffolds with pore structures and geometries akin to those of the *Pitta moluccensis* humerus. This approach not only bridges the gap between natural and synthetic biomaterials but

*Corresponding author:
Tel : 13461862704
Fax: 03963690378
E-mail: czqjuan@126.com

also advances the development of tailored solutions for orthopedic and tissue engineering applications.

Materials and Methods

Samples of bird humerus bone (sterilized in alcohol) and demineralized bone matrix (treated for 2 hours in 0.5 M HCl) were obtained from a biological sample repository. The samples were selected from donors in good health conditions with no significant pathological history. Silicon nitride (Si3N4)-based samples were fabricated using a replica method with polyurethane sponges serving as pore-forming agents. A suspension containing 35 vol% of Si_3N_4 powder (d_{90} = 10.0 μm, Yantai, Tomley Hi-Tech Ind. & Tra. Co., Ltd.) was prepared using deionized water as the liquid medium. A dispersant (0.022 g per gram of powder) was added to enhance suspension stability, followed by 24-hour homogenization through ball milling using Si_3N_4 milling balls. Polyurethane sponges were immersed in the slurry and compressed to ensure full infiltration of the pores and good wetting between the sponge and the slurry. Excess suspension was removed by passing the impregnated sponges through rollers. After drying, the sponges were burned out at 600 °C for 1 hour in air (heating rate: 1 °C/min). The samples were subsequently sintered in air at 1250 °C using a heating rate of 10 °C/min and a cooling rate of 20 °C/min.The volumetric image series of X-ray computed tomography (CT/microCT) used in this study were adopted from Morphosource, with data access provided by Doug Boyer under NSF BCS 1317525 and NSF BCS 1552848

The analysis of the *Pitta moluccensis* humerus bone using X-ray computed tomography (CT/microCT) provides valuable insights into its microstructural architecture, essential for understanding its mechanical properties and potential as a reference in biomaterial design. The images adopted from Morphosource showcase the intricate trabecular network characteristic of avian bone, offering an exceptional model for biomimetic studies. The CT/microCT slice images reveal a highly porous structure with interconnected trabeculae. The porosity, quantified at approximately 70 vol%, contributes to the lightweight yet robust nature of the *Pitta moluccensis* humerus, making it well-suited for flight. The trabecular spacing and thickness observed in the images exhibit uniformity, indicative of optimal load distribution during avian locomotion. The pore diameters, ranging from sub-micrometer to several micrometers, are consistent with the measurements derived from mercury intrusion porosimetry. These microstructural characteristics serve as benchmarks for designing biomimetic materials like silicon nitride ceramics. The trabecular orientation, as visualized in the CT/microCT slices, aligns predominantly along the longitudinal axis of the bone (Fig. 2). This alignment optimizes the bone's resistance to compressive and bending forces during flight. Such insights emphasize the importance of directional porosity in the design of synthetic bone substitutes, as it directly influences mechanical strength and load-bearing capabilities.

When comparing the microstructure of the humerus bone to silicon nitride ceramics prepared via the replica method, several parallels can be drawn. The pore size

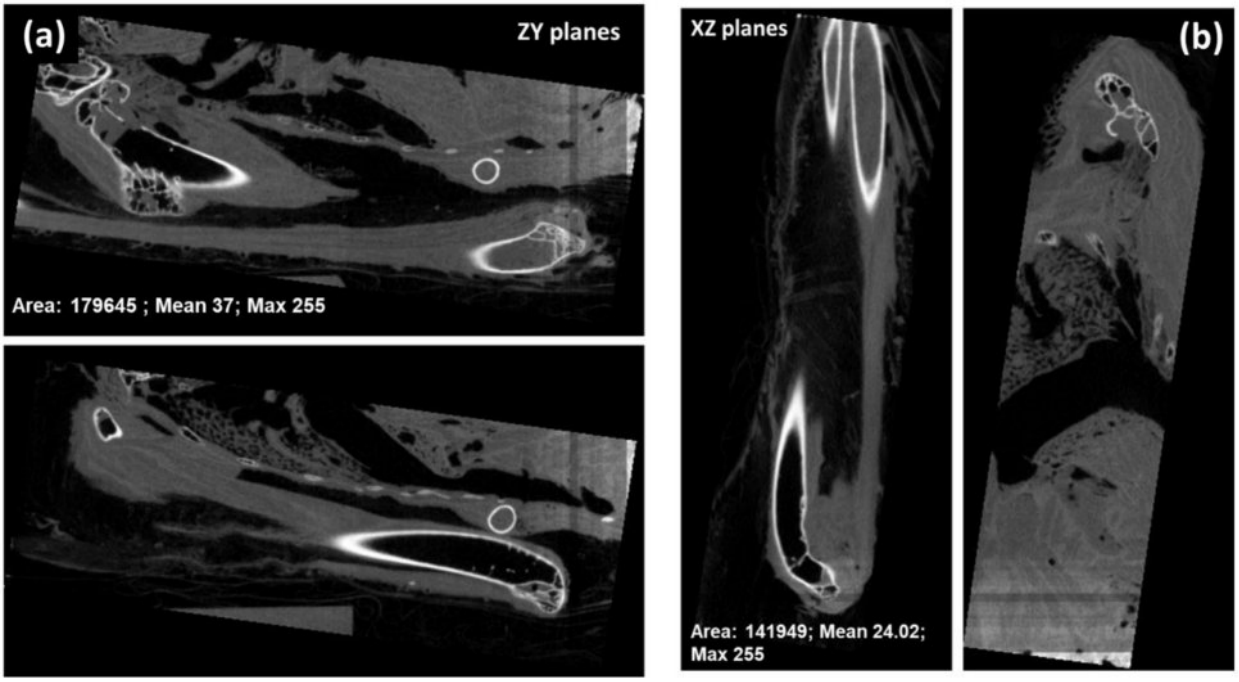

Fig. 1. Slice image of X-ray computed tomography (CT/microCT) of the *Pitta moluccensis* humerus bone, adopted from Morphosource. Data courtesy of Doug Boyer under NSF BCS 1317525 and NSF BCS 1552848.

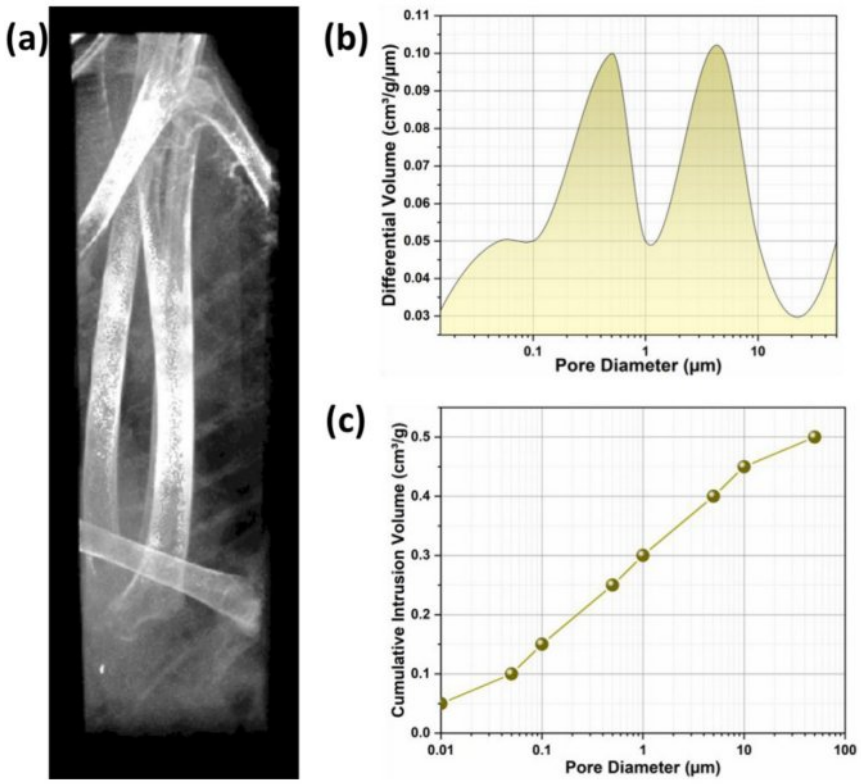

Fig. 2.

distribution in the silicon nitride samples mimics the natural trabecular architecture of the humerus bone, with pores ranging from 0.1 to 50 µm. This similarity enhances the material's suitability for bone substitution by promoting mechanical compatibility and biointegration. The high-resolution CT/microCT images also highlight the thin cortical shell surrounding the trabecular core, a feature that adds structural rigidity while maintaining a lightweight profile. This dual property is mimicked in silicon nitride ceramics through controlled sintering and porosity optimization, making them an ideal candidate for applications requiring load-bearing implants.

The pore size distribution analysis is crucial in comparing the natural porosity of the humerus bone of *Pitta moluccensis* with synthetic Si_3N_4 ceramics. The differential volume vs. pore diameter graph provides detailed insights into the specific pore size contributions (Fig. 2a and 3a). For the *Pitta moluccensis* humerus bone, the differential volume shows two distinct peaks at 0.50 µm (0.10 $cm^3/g/\mu m$) and 5.0 µm (0.10 $cm^3/g/\mu m$). These peaks suggest that the majority of the porosity of the bone is concentrated in these size ranges, correlating with its structural role in providing strength and facilitating fluid transport. In Si_3N_4 a broader distribution is evident, with a prominent peak at 100 µm (0.90 $cm^3/g/\mu m$). The highest differential volume values occur in the larger pore size range (50-200 µm), which could enhance osteointegration by mimicking the natural bone environment. The second peak at 10 µm (0.68 $cm^3/g/\mu m$) corresponds to microporosity that supports nutrient exchange and cell adhesion.

The cumulative intrusion volume vs. pore diameter graph demonstrates the extent of pore infiltration across various pore sizes (Fig. 2b and 3b). For the *Pitta moluccensis* humerus bone, the cumulative intrusion volume increases progressively, reaching a maximum of 0.50 cm^3/g at a pore diameter of 50 µm. The largest increase is observed between 0.50 µm (0.25 cm^3/g) and 5.0 µm (0.40 cm^3/g), indicating the dominance of pores within this range. In contrast, the silicon nitride ceramics exhibit a broader range of pore sizes. The cumulative intrusion volume peaks at 0.50 cm^3/g at a pore diameter of 10 µm, followed by a gradual decline as pore sizes increase. The volume sharply increases in the smaller pore range, particularly from 0.1 µm (0.01 cm^3/g) to 10 µm (0.50 cm^3/g), suggesting a higher contribution of microporosity. This difference highlights the controlled fabrication of Si_3N_4 ceramics, ensuring a uniform distribution of micropores for enhanced mechanical properties. However, the humerus bone demonstrates a narrower pore size distribution, emphasizing its biological adaptation for lightweight strength and vascularization. The narrow pore size range in the humerus bone reflects its optimized structure for mechanical and biological performance, with a significant focus on mid-sized pores (0.5-10 µm). Silicon nitride ceramics, with their broader pore distribution, offer versatility in tailoring properties for specific applications. For instance, the presence

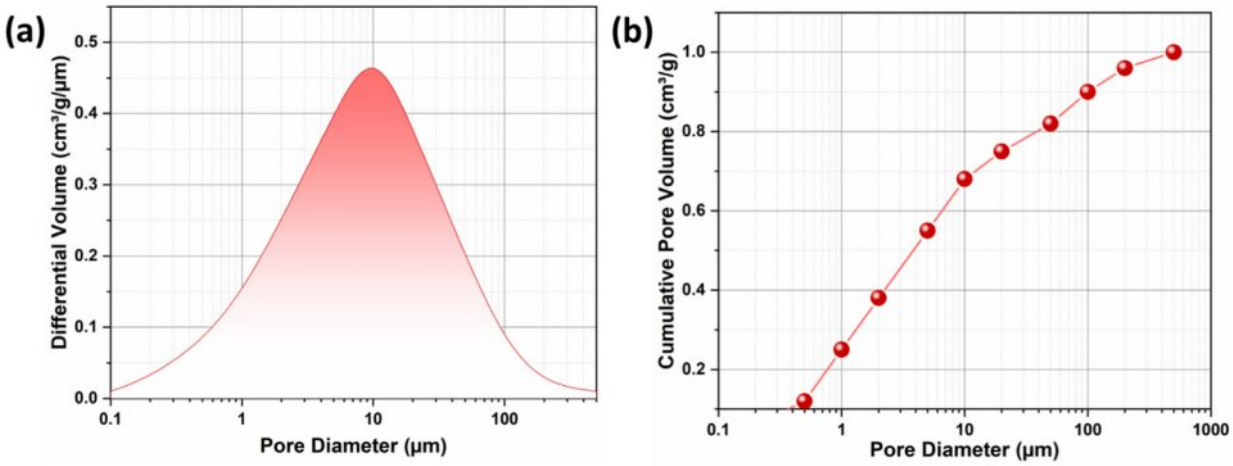

Fig. 3. Differential volume and Cumulative intrusion volume as a function of pore diameter for the Si_3N_4 ceramics.

of large pores in Si_3N_4 ceramics facilitates enhanced vascularization and tissue ingrowth, while smaller pores mimic the bone matrix's ability to support osteoblast proliferation. However, the mismatch in peak pore sizes (5 μm for bone vs. 100 μm for Si_3N_4) may necessitate modifications in Si_3N_4 fabrication methods, such as adjusting the slurry composition or sintering conditions, to better match natural bone porosity.

Mechanical Properties and Relevance to Bone Substitutes

The mechanical properties of the humerus bone of *Pitta moluccensis* and air-sintered silicon nitride ceramics are summarized based on experimental analysis. These properties were evaluated using a nano-indentation technique, ensuring the measurements reflected the intrinsic characteristics of the bone and ceramic matrix without accounting for the influence of large pores or skeletal structures. The Si_3N_4 samples demonstrated mechanical properties comparable to those of the bone matrix. Specifically, the hardness of the Si_3N_4 was measured at 0.4 GPa, closely aligning with the measured hardness of the *Pitta moluccensis* humerus bone, which was 0.3 GPa. The Young's modulus of the Si_3N_4 samples was 15 GPa, slightly higher but still within a reasonable range of the bone matrix value of 12 GPa. This similarity is attributed to the tailored porosity and the microstructural characteristics of silicon nitride ceramics, which mimic the natural architecture of trabecular bone. The compressive strength of the air-sintered silicon nitride ceramics was determined to be 2.9±0.4 MPa, which is slightly lower than the 3.5 MPa measured for the *Pitta moluccensis* humerus bone. Despite this slight difference, the values are within the acceptable range for biomaterials intended for trabecular bone substitution. The observed compressive strength is a result of the interconnected porosity in the Si_3N_4 samples, which balances mechanical stability with the ability to facilitate nutrient transport and vascularization. The porosity of the ceramics (~50 vol%) closely matches that of the humerus bone (~70 vol%), reinforcing their potential for biointegration.

The similarity in mechanical properties between Si_3N_4 ceramics and the humerus bone of *Pitta moluccensis* underscores their suitability as a bone substitute. It is noteworthy, however, that slight discrepancies in elastic modulus or strength between the bone and ceramic materials could lead to stress concentration at the bone–ceramic interface. Addressing this challenge may require further optimization, such as adjusting the sintering temperature or refining the porosity to achieve even closer mechanical compatibility. Compared to other ceramic biomaterials, such as Al_2O_3 and ZrO_2, silicon nitride offers the added advantage of osteoconductive and antibacterial properties. This positions it as a promising material for bone tissue engineering, particularly in applications requiring lightweight and mechanically resilient substitutes.

Conclusion

This study demonstrates that Si_3N_4 ceramics exhibit mechanical and structural properties comparable to the demineralized humerus bone of *Pitta moluccensis*, making them promising candidates for bone substitution. The ceramics displayed a hardness of 0.4 GPa, a Young's modulus of 15 GPa, and a compressive strength of 2.9±0.4 MPa, similar to the bird bone's 0.3 GPa, 12 GPa, and 3.5 MPa, respectively. The Si_3N_4 ceramics also exhibited a porosity of ~50 vol%, closely matching the ~70 vol% in the bird bone, which enhances their mechanical compatibility and potential for biointegration. Despite minor differences in mechanical properties, Si_3N_4 ceramics show significant promise as lightweight, durable, and biocompatible materials for orthopedic implants, with potential for further optimization in fabrication methods.

References

1. S. Liu, F. Ye, L. Liu, and Q. Liu, Mater. Design 16 (2015) 331-335.
2. R. Zou, L. Bi, Y. Huang, Y. Wang, Y. Wang, L. Li, J. Liu, L. Feng, X. Jiang, and B. Deng, J. Mech. Behav. Biomed. Mater. 141 (2023) 105756.
3. S. Zhao, W. Xiao, M.N. Rahaman, D. O'Brien, J.W. Seitz-Sampson, and B.S. Bal, Int. J. Appl. Ceram. Technol. 14[2] (2017) 117-127.
4. W.D. Rao, Y. Liu, L.J. Cheng, and S.J. Liu, J. Cent. South Univ. 28[4] (2021) 1233-1243.
5. X. Li, L. Zhang, and X. Yin, Script Mater 67[4] (2012) 380-383.
6. C. Santos, I.F. Coutinho, J.E.V. Amarante, M.F.R.P. Alves, M.M. Coutinho, and C.R.M. Silva, J. Mech. Behav. Biomed. 116 (2021) 104372.
7. Q. Zhou, X. Su, J. Wu, X. Zhang, R. Su, L. Ma, Q. Sun, and R. He, ACS Biomater. Sci. Eng. 9[3] (2023) 1164-1189.
8. L. Huang, Y. Dong, Z. Wang, D. Zhang, and Z. Yu, Int. J. Refract. Met. Hard Mater. 125 (2024) 106907.
9. A. Sharama, A. Babbar, Y. Tian, B. P. Pathri, M. Gupta, and R. Singh, Int. J. Interact. Des. Manuf. 17 (2022) 2891-29N.
10. Vidakis, M. Petousis, N. Michailidis, V. Papadakis, N. Mountakis, A. Argyros, E. Dimitriou, C. Charou, and A. Moutsopoulou, Adv. Biomed. Eng. 6 (2023) 10010311.